

Light Neutralino Dark Matter in the NMSSM

Qiurong Mou,^{1,*} Hongyan Wu,^{1,†} and Sibozheng^{1,‡}

¹*Department of Physics, Chongqing University, Chongqing 401331, P. R. China*

(Dated: February 21, 2018)

Abstract

The next-to-minimal supersymmetric standard model can host light neutralino dark matter with mass of order GeV scale. It is dominated by the singlino component as a result of approximate Peccei-Quinn symmetry. This paper is devoted to address the question how light such neutralino dark matter can be in the light of the LHC Run 1 data as well as the latest LUX and Xenon1T limits. In particular, we show the sensitivity of parameter space of dark matter mass with respect to Z boson and SM Higgs invisible decay.

arXiv:1703.00343v5 [hep-ph] 21 Feb 2018

*Electronic address: qiurongmou@163.com

†Electronic address: hongyanwu@cqu.edu.cn

‡Electronic address: sibozheng.zju@gmail.com

I. INTRODUCTION

It is well known that the Standard Model (SM)-like Higgs discovered at the LHC [1, 2] imposes severe constraint on stop soft mass parameters. They are at least several TeVs in order to provide significant radioactive correction to Higgs mass [3–5] in the situation of small mixing or of small tree-level modification. Similar favor to large soft masses for the others such as gluino mass is also suggested by the LHC Run 1 data.

When the soft mass parameters of supersymmetry are large (in compared with the weak scale), it is hardly available to directly detect them at the LHC, unless some of dimensionless parameters of supersymmetry are extremely large or small. Such specific choices reopen the potential of leaving striking signatures in collider or astrophysical experimental facilities.

In supersymmetric models favored by simplicity, the Minimal Supersymmetric Standard Model (MSSM) and the Next-to-Minimal Supersymmetric Standard Model (NMSSM) (For a review, see, e.g., [6]) are the two simplest ones which retain the unification [7] of SM gauge coupling constants. The later one is an extension of the former by adding a singlet S with superpotential

$$W = \lambda S H_u H_d + \frac{\kappa}{3} S^3. \quad (1)$$

The dimensionless parameters in the NMSSM are thus composed of λ and κ of Eq.(1). Following previous line it is prior to tune λ or κ in the sense that it may leave detectable signatures and help us distinguish NMSSM from MSSM simultaneously.

Remarkably, a small value of κ yields a singlino-like neutralino dark matter (DM) with mass as light as a few GeVs. The smallness of κ can be simply analyzed as an input parameter as in earlier studies [8–19]. Alternatively, it is a result of approximate Peccei-Quinn (PQ) symmetry¹ as we choose here. Unlike in the large mass region, a light DM is rather sensitive to Z boson [20–22] and Higgs [23, 24] invisible decay limits. Consider that the later one will be significantly improved in comparison with earlier studies, it is meaningful to uncover the sensitivity of parameter space of DM mass to this experimental value.

The plan of this paper is organized as follows. In Sec.2 we firstly analyze the mass matrixes and interactions under the approximate PQ symmetry both in the Higgs and neutralino sector. Then we use the numerical code NMSSMTools 5.0.2 [25] to solve eigenstate masses, and micrOMEGAs [26] to extract parameter space imposed by DM relic abundance as well as direct detection limits at LUX [27, 28] and Xenon1T [29, 30]. Sec.3 is devoted to DM indirect detections at particle colliders. We show the constraints arising from Z boson [32] and latest Higgs [33] invisible decay at the LHC. Finally, we conclude in Sec.4. The appendix is added to introduce our convention and notations.

¹ If κ term vanishes the Lagrangian would be invariant under the following $U(1)$ symmetry transformation,

$$H_u \rightarrow H_u \exp(i\phi), \quad H_d \rightarrow H_d \exp(i\phi), \quad S \rightarrow S \exp(-2i\phi).$$

II. LIGHT SINGLINO DARK MATTER IN NMSSM

The neutralino DM is dominated by the singlino component in PQ-symmetric NMSSM, as inferred from the neutralino mass matrix in Eq.(A4). The DM mass eigenvalue is generally handled by numerical calculation. In contrast, analytic approximations can be only obtained under the decoupling limit $M_{1,2} \gg \mu$, which are useful for illustrating the numerical results in the text. When the wino and bino are decoupled in Eq.(A4), the remaining three mass eigenstates ordered in mass are then decomposed as,

$$\tilde{\chi}_i^0 \simeq N_{i3}\tilde{H}_u + N_{i4}\tilde{H}_d + N_{i5}\tilde{s}, \quad (2)$$

where N is a unitary matrix to diagonalize the remaining neutralino mass M_χ . The matrix elements in Eq.(2) are approximated by [34],

$$N_{i3} : N_{i4} : N_{i5} \simeq \lambda(\mu v_u - v_d m_{\tilde{\chi}_i^0}) : \lambda(\mu v_d - v_u m_{\tilde{\chi}_i^0}) : (m_{\tilde{\chi}_i^0}^2 - \mu^2), \quad (3)$$

where $m_{\tilde{\chi}_i^0}$ refers to the mass of $\tilde{\chi}_i^0$.

A. Relic Abundance

The relic abundance of thermal DM is determined by the averaged annihilation cross section $\langle\sigma v\rangle$ at the freeze-out time, which is mainly given by the annihilation of singlino to $\tau\tau$ or $b\bar{b}$ through the light CP odd scalar A_1 if kinetically allowed. As shown in [17] it is approximated as,

$$\langle\sigma v\rangle \simeq \frac{g_2^2 c_f}{8\pi} \frac{m_f^2}{M_W^2} \cos^2 \theta_A \tan^2 \beta \times |T_{A_1 \tilde{\chi}_1^0 \tilde{\chi}_1^0}|^2 \times \frac{m_{\tilde{\chi}_1^0}^2 \sqrt{1 - m_f^2/m_{\tilde{\chi}_1^0}^2}}{(4m_{\tilde{\chi}_1^0}^2 - m_{A_1}^2)^2 + m_{A_1}^2 \Gamma_{A_1}^2}, \quad (4)$$

where $c_f = 1(3)$ for lepton (quark), m_f is the SM fermion mass, $T_{A_1 \tilde{\chi}_1^0 \tilde{\chi}_1^0}$ denotes the the CP-odd Higgs-neutralino-neutralino coupling, m_{A_1} is the lighter CP-odd scalar mass, and $\cos \theta_A$ refers to the mixing angle between the CP-odd scalar A of MSSM and S_I of the singlet. The magnitude of $T_{A_1 \tilde{\chi}_1^0 \tilde{\chi}_1^0}$ reads as

$$T_{A_1 \tilde{\chi}_1^0 \tilde{\chi}_1^0} \simeq \sqrt{2}\lambda \cos \theta_A N_{15}(N_{13} \sin \beta + N_{14} \cos \beta) + \sqrt{2} \sin \theta_A (\lambda N_{13} N_{14} - \kappa N_{15}^2). \quad (5)$$

We refer the reader to the appendix for the other parameters in Eq.(4). One obtains the estimate of relic abundance by substituting Eq.(4) into the standard formula,

$$\Omega_{\tilde{\chi}_1^0} h^2 \simeq \frac{10^9 \text{GeV}^{-1}}{M_P} \frac{x_F}{\sqrt{g_*}} \frac{1}{\langle\sigma v\rangle}, \quad (6)$$

where M_P is the Planck mass, $x_F \sim 20$, and g_* is effective number of freedoms at the freeze-out temperature. The experimental value of DM relic abundance reported by Planck and WMAP [36] is given as

$$\Omega_{\tilde{\chi}_1^0} h^2 = 0.1197 \pm 0.0022. \quad (7)$$

Parameter range
$0.1 \leq \lambda \leq 0.7$
$5 < \tan \beta \leq 30$
$0.005 \leq \kappa \leq 0.07$
$103 \leq \mu \leq 500$
$-2000 \leq A_\lambda \leq 2000$
$-500 \leq A_\kappa \leq 500$
$100 \leq M_{1,2} \leq 1000$
$1000 \leq M_3 \leq 2500$
$-3000 \leq A_{t,b} \leq 3000$
$800 \leq m_{\tilde{t},\tilde{b}} \leq 2000$

TABLE I: Scanned parameter ranges, where soft mass parameters are in unit of GeV. Large gluino and stop masses are chosen by referring their lower bounds at the LHC (~ 1.5 TeV and ~ 740 GeV for gluino and stop, respectively [35]) whereas small κ is adopted in the spirit of spontaneously broken PQ symmetry.

Obviously, the parameter space induced by DM relic density is sensitive to the two mixing angles and masses of DM and light CP-odd scalar in Eq.(4), which are directly related to parameters λ , $\tan \beta$, κ , μ , A_λ and A_κ as shown in the appendix, and indirectly to parameters such as gaugino masses M_i as well as the soft masses involving the third generation. The parameter ranges for them to be scanned in terms of the numerical codes NMSSMTools 5.0.2 [25] and micrOMEGAs [26] are explicitly shown in Table.I. What is the most different in our scans of parameter ranges from the other studies in the literature is that large gluino and stop masses are chosen whereas small κ is adopted in the spirit of spontaneously broken PQ symmetry.

Apart from constraints contained in the code, there are 2560 out of 20 million samples in this scan which satisfy DM relic density and SM Higgs mass constraint simultaneously. In Fig.1 we show the parameter space in two different ways. The left plot reveals the dependence of N_{1i} ($i = 3 - 5$) on the DM mass, which verifies that the singlino component is indeed the main component. The right plot indicates the coherence of masses of DM and the lighter CP-odd scalar, where they trend to saturate at the resonant annihilation $m_{A_1} = 2m_{\tilde{\chi}_1^0}$, especially for DM mass beneath half of m_Z . The reason is that the coefficient of $T_{A_1\tilde{\chi}_1^0\tilde{\chi}_1^0}$ and that of mixing angle in Eq.(4) are both small in this DM mass region. A resonant annihilation is therefore needed to compensate the suppression. But it is modified when the lightest CP-even Higgs h_1 makes substantial contribution to the singlino annihilation.

B. Direct Detection

Since samples which satisfy the DM relic density have been prepared, it is straightforward to discuss DM direct detection in terms of DM-nucleon scattering. The spin-independent (SI) and spin-dependent (SD) scattering cross section σ is given by Feynman diagram of interchanging SM Higgs and Z boson, respectively. By employing micrOMEGAs [26] we show σ_{SI} and σ_{SD} as function of DM mass $m_{\tilde{\chi}_1^0}$ in the left and right plot of Fig.2, respectively.

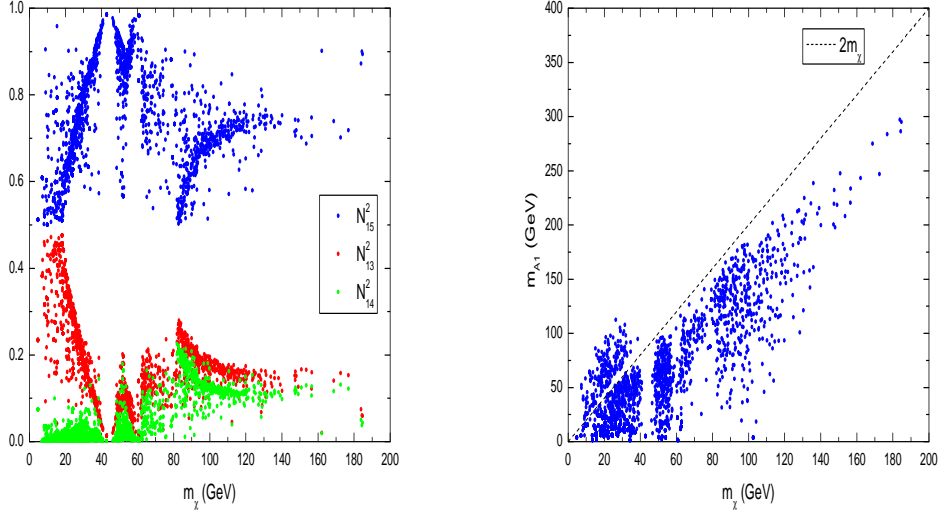


FIG. 1: Samples which satisfy DM relic abundance [36], $N_{15}^2 \geq 0.5$ and Higgs mass $m_{h_2} = 125.1 \pm 1.0$ GeV. Left plot: the parameter space is projected to the two-parameter plane of DM mass and N_{15}^2 , with $|N_{13}|^2$ and $|N_{14}|^2$ shown for illustration. Right plot: It is projected to two-parameter plane of masses of DM and lighter CP-odd scalar, where the dotted line refers to the resonant mass relation $m_{A_1} = 2m_{\tilde{\chi}_1^0}$.

In the left plot samples referred by “•” and by “×” are excluded by the SI limits at LUX [27] and Xenon1T [29], respectively. Nevertheless, samples referred by “△” are still consistent with these SI limits. Meanwhile, exclusions by different SD limits are also illustrated by different colors in the left plot, with blue and green corresponding to Xenon1T [30] and LZ [31], respectively, as clearly shown in the right plot. Therefore, sample referred by red “△” are consistent with both nowadays SI and SD limits, although the number of them is rare in the figure.

The left plot of Fig.2 shows that most of samples have been excluded by SI limit at LUX. The main reason is that σ_{SI} is approximated to be

$$\sigma_{SI} = \frac{4}{\pi} \left(\frac{m_{\tilde{\chi}_1^0} m_p}{m_{\tilde{\chi}_1^0} + m_p} \right)^2 f_p^2, \quad (8)$$

for moderate or large value of $\tan \beta$. Here, m_p is the proton mass, and f_p is given by

$$\frac{f_p}{m_p} \simeq \frac{g}{4M_W m_h^2} T_{h_2 \tilde{\chi}_1^0 \tilde{\chi}_1^0} \cdot (f_{Td} - f_{Tu} + f_{Ts} - \frac{2}{27} f_{TG}) \simeq 7 \times 10^{-3} \frac{g}{4M_W m_h^2} T_{h_2 \tilde{\chi}_1^0 \tilde{\chi}_1^0}, \quad (9)$$

with

$$T_{h_2 \tilde{\chi}_1^0 \tilde{\chi}_1^0} \simeq \sqrt{2} \lambda N_{15} (N_{13} \cos \beta + N_{14} \sin \beta). \quad (10)$$

The magnitude of $T_{h_2 \tilde{\chi}_1^0 \tilde{\chi}_1^0}$ is typically of order $10^{-1} - 10^{-2}$. Substituting Eq.(10) into Eq.(8) gives rise to σ_{SI} typically of order 10^{-8} pb, which is excluded by the latest LUX 2016 limit

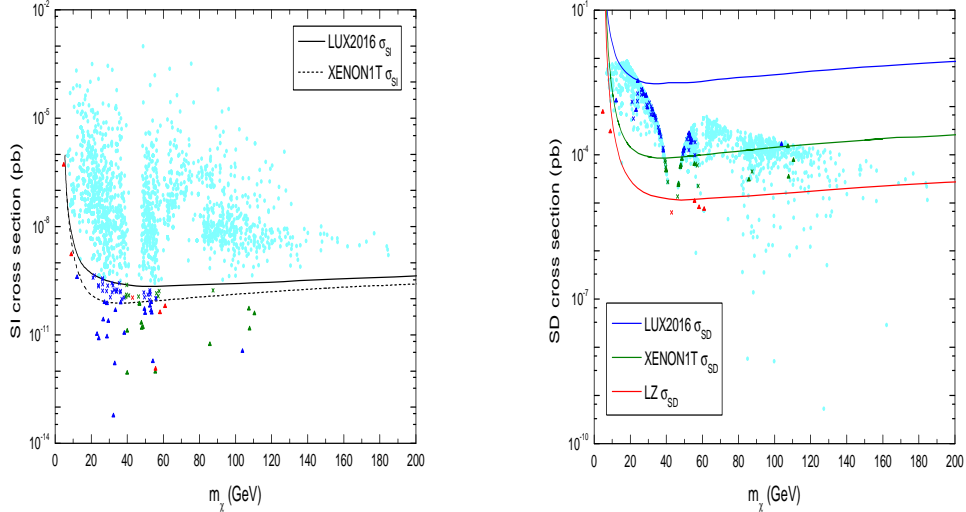


FIG. 2: SI (left) and SD (right) cross section for the same samples of Fig.1. What are referred by “•” and “×” are excluded by the SI limits at LUX [27] and Xenon1T [29], respectively; and by blue and green are excluded by the SD limit at Xenon1T [30] and LZ [31], respectively. In contrast, samples marked by red “△” are not excluded neither by SD or SI limits.

[27]. σ_{SI} can further decrease when the signs of N_{13} and N_{14} are opposite, as a result of which $T_{h_2\tilde{\chi}_1^0\tilde{\chi}_1^0}$ in Eq.(10) is significantly suppressed to help evade the LUX or even Xenon1T limit.

III. COLLIDER CONSTRAINTS

Results in the previous section show that light neutralino DM still survives in the facilities of LUX, Xenon1T and LZ. It is natural to ask what the fate of them is at colliders. This section is devoted to explore this question.

Before we address the constraint imposed by Z boson invisible decay into light neutralino DM, we postpone the discussion about Higgs invisible decay. The invisible decay width Γ_Z^{inv} is determined by [37],

$$\Gamma_Z^{\text{inv}} = \frac{G_F M_Z^3}{12\sqrt{2}\pi} (N_{13}^2 - N_{14}^2)^2 \left(1 - \frac{4m_{\tilde{\chi}_1^0}^2}{M_Z^2}\right)^{3/2} \simeq 0.165 \text{ GeV} \cdot (N_{13}^2 - N_{14}^2)^2, \quad (11)$$

The reported experimental bound $\Gamma_Z^{\text{inv}} \leq 2 \text{ MeV}$ [32] implies that the magnitude of $(N_{13}^2 - N_{14}^2)^2$ in Eq.(11) is upper bounded by ~ 0.01 roughly. It explains why most of samples in Fig.1 are excluded according to the left plot therein. Fortunately, the left plot of Fig.3 shows that a small portion of samples (red triangle) surviving in DM direct detection experiments is still not ruled out by this bound.

Finally, we discuss the constraint arising from SM Higgs invisible decay. Since light A_1 is needed by light singlino-like DM, the invisible decay width Γ_h^{inv} may be composed of the

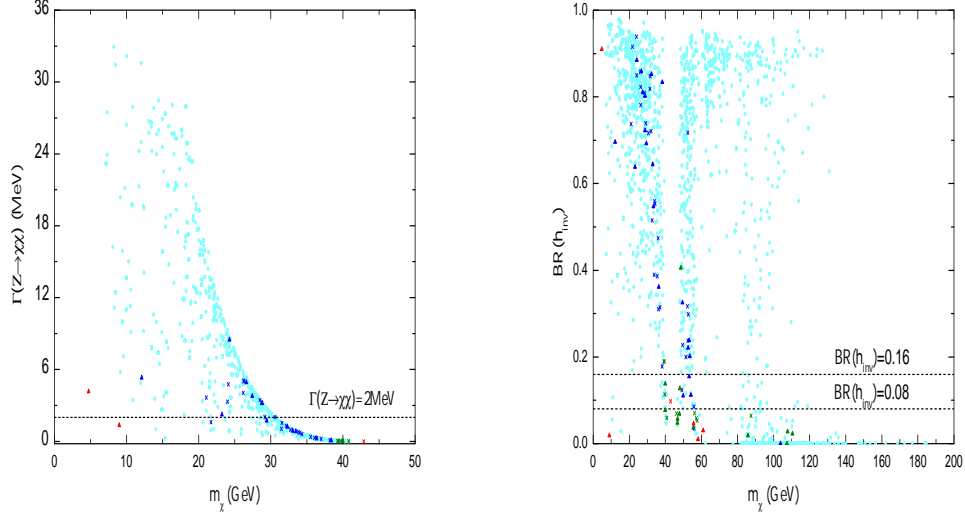


FIG. 3: Left plot: contribution to Z boson invisible decay for the same samples of Fig.1, where it tells us that the reported upper bound on $\Delta\Gamma_Z$ [32] has already imposed severely constraint on the parameter space. Right plot: contribution to SM Higgs invisible decay instead, where the horizontal dotted line from top to bottom refers to $\Gamma_h^{inv}/\Gamma_h = \{0.16, 0.08\}$ respectively. Note that the reference of colors in these two plots are the same as that of Fig.2.

following three parts :

$$\begin{aligned}
\Gamma(h_2 \rightarrow h_1 h_1) &= \frac{1}{16\pi m_{h_2}} |T_{h_2-h_1-h_1}|^2 \left(1 - \frac{4m_{h_1}^2}{m_{h_2}^2}\right)^{1/2}, \\
\Gamma(h_2 \rightarrow \tilde{\chi}_1^0 \tilde{\chi}_1^0) &= \frac{1}{8\pi} |T_{h_2-\tilde{\chi}_1^0-\tilde{\chi}_1^0}|^2 m_h \left(1 - \frac{4m_{\tilde{\chi}_1^0}^2}{m_{h_2}^2}\right)^{3/2}, \\
\Gamma(h_2 \rightarrow A_1 A_1) &= \frac{1}{16\pi m_{h_2}} |T_{h_2-A_1-A_1}|^2 \left(1 - \frac{4m_{A_1}^2}{m_{h_2}^2}\right)^{1/2}.
\end{aligned} \tag{12}$$

Eq.(12) suggests that Γ_h^{inv} is very sensitive to the Yukawa coefficients T s. Similar to Γ_Z^{inv} the upper bound $\Gamma_h^{inv} \leq 16\% \cdot \Gamma_h$ [33] as reported in the LHC Run 1 data has also excluded most of samples. When DM mass is above half of SM Higgs mass, the second channel in Eq.(12) is closed, but the others may be still allowed. After combing the plots of Fig.2 we draw the conclusion that neutralino DM with mass as light as several GeVs is hardly excluded by the Z boson and Higgs invisible decay. In Table.II we show the main input and out parameters of a benchmark point.

λ	κ	$\tan\beta$	μ	M_3	$m_{\tilde{t}_3}$	A_t	m_{h_3}	m_{h_2}	m_{h_1}	m_{A_2}	m_{A_1}	$m_{\tilde{\chi}_1^0}$	Γ_Z^{inv}	Br_h^{inv}
0.32	0.007	9.67	172.87	1708.15	1368.64	-2674.69	1687.88	125.18	25.81	1687.85	21.09	8.98	1.35	1.9%

TABLE II: Main input parameters and output mass spectrum for a benchmark point in Fig.3, where mass and Γ_Z^{inv} is in unit of GeV and MeV, respectively.

IV. CONCLUSION

This work presented a numerical study of NMSSM with heavy soft mass parameters associated with the third generation but light neutralino DM due to small spontaneously breaking of PQ symmetry. Naively speaking, such light DM may be already excluded either by DM direct detection facilities or SM Z boson and Higgs scalar invisible decay experiments. The main finding, however, is that both the latest SD and SI limits from LUX and Xenon1T are unable to exclude light neutralino DM with mass of order several GeVs. This study also demonstrates that even the further precision test on Higgs invisible decay at the HL-LHC or LZ experiments fail to exclude such a possibility.

Acknowledgments

This work is supported in part by the National Natural Science Foundation of China under Grant No.11775039.

Appendix A: Mass Matrixes

The mass matrixes discussed in this appendix determine both the DM eigenstate mass and its couplings to CP-even Higgs scalar, CP-odd scalar A_1 , Z boson etc. Firstly, we follow Ref. [38] to decompose the Higgs doublet scalars $H_{u,d}^0$ and singlet scalar S into the following fields,

$$\begin{aligned}
H_u^0 &= v_u + \frac{1}{\sqrt{2}}(H_{uR} + iH_{uI}), \\
H_d^0 &= v_d + \frac{1}{\sqrt{2}}(H_{dR} + iH_{dI}), \\
S &= s + \frac{1}{\sqrt{2}}(S_R + iS_I),
\end{aligned} \tag{A1}$$

where $v_u^2 + v_d^2 = (174 \text{ GeV})^2$ and s is the vacuum expectation value of singlet scalar. In order to eliminate the Goldstone mode, one rotates the gauge eigenstates from (H_{uR}, H_{dR}, S_R) to (H, h, S_R) via the orthogonal matrix $U(\beta)$ with $\tan\beta = v_u/v_d$. Under the new basis (H, h, S_R) , the CP-even mass squared reads as,

$$\mathcal{M}_S^2 = \begin{pmatrix} \frac{A_\lambda^2}{1+x} + (M_Z^2 - \lambda^2 v^2) \sin^2 2\beta & -\frac{1}{2}(M_Z^2 - \lambda^2 v^2) \sin 4\beta & -\lambda A_\lambda v \cos 2\beta \\ * & M_Z^2 \cos^2 2\beta + \lambda^2 v^2 \sin^2 2\beta & -\lambda A_\lambda v \sin 2\beta \frac{x}{1+x} \\ * & * & \lambda^2 v^2 (1+x) \end{pmatrix} \tag{A2}$$

Here $x = m_s^2/(\lambda^2 v^2)$. After diagonalization by an orthogonal matrix S_{ij} we obtain three CP-even neutral scalars h_i , and one of them is identified as the SM-like Higgs. The off-diagonal elements in M_S^2 determine the mixing effects between these mass eigenstates, the magnitude of which are severely upper bounded by the Higgs precision measurements at the LHC [39]. With small mixing effects the SM-like Higgs is mainly composed of h_2 .

Under basis (A, S_I) the mass matrix squared for CP-odd scalars is given by,

$$\mathcal{M}_P^2 \simeq \begin{pmatrix} \frac{2\mu}{\sin 2\beta} A_\lambda & \lambda v A_\lambda \\ * & \frac{\lambda^2 v^2 A_\lambda \sin 2\beta}{2\mu} \end{pmatrix} \quad (\text{A3})$$

After diagonalization by an orthogonal 2×2 matrix $P'_{ij}(\theta_A)$ with angle θ_A , one obtains two CP-odd neutral scalars A_i (ordered in mass). The determinant of \mathcal{M}_P^2 in Eq.(A3) is zero in the PQ limit, which implies that there is a massless CP-odd scalar.

On the other hand, the neutralino mass matrix M_χ under the gauge eigenstates $(\tilde{B}, \tilde{W}, \tilde{H}_u, \tilde{H}_d, \tilde{s})$ are given by,

$$M_\chi = \begin{pmatrix} M_1 & 0 & M_Z s_W \sin \beta & -M_Z s_W \cos \beta & 0 \\ * & M_2 & -M_Z c_W \sin \beta & M_Z c_W \cos \beta & 0 \\ * & * & 0 & -\mu & -\lambda v_d \\ * & * & -\mu & 0 & -\lambda v_u \\ * & * & * & * & \frac{2\kappa}{\lambda} \mu \end{pmatrix}, \quad (\text{A4})$$

where $\mu = \lambda s$ and $s_W = \sin \theta_W$. When $M_1, M_2 \gg \mu$, bino and wino are decoupled, which leads to a singlino-like neutralino LSP.

-
- [1] G. Aad *et al.* [ATLAS Collaboration], Phys. Lett. B **716**, 1 (2012), [arXiv:1207.7214 [hep-ex]].
 - [2] S. Chatrchyan *et al.* [CMS Collaboration], Phys. Lett. B **716**, 30 (2012), [arXiv:1207.7235 [hep-ex]].
 - [3] M. Carena, S. Gori, N. R. Shah and C. E. M. Wagner, JHEP **1203**, 014 (2012), [arXiv:1112.3336 [hep-ph]].
 - [4] L. J. Hall, D. Pinner and J. T. Ruderman, JHEP **1204**, 131 (2012), [arXiv:1112.2703 [hep-ph]].
 - [5] J. J. Cao, Z. X. Heng, J. M. Yang, Y. M. Zhang and J. Y. Zhu, JHEP **1203**, 086 (2012), [arXiv:1202.5821 [hep-ph]].
 - [6] U. Ellwanger, C. Hugonie and A. M. Teixeira, Phys. Rept. **496**, 1 (2010), [arXiv:0910.1785 [hep-ph]].
 - [7] S. Zheng, Eur. Phys. J. C **77**, no. 9, 588 (2017), [arXiv:1706.01071 [hep-ph]].
 - [8] J. Cao, Y. He, L. Shang, W. Su, P. Wu and Y. Zhang, JHEP **1610**, 136 (2016), [arXiv:1609.00204 [hep-ph]].
 - [9] Q. F. Xiang, X. J. Bi, P. F. Yin and Z. H. Yu, Phys. Rev. D **94**, no. 5, 055031 (2016), [arXiv:1606.02149 [hep-ph]].
 - [10] M. Badziak, M. Olechowski and P. Szczerbiak, JHEP **1603**, 179 (2016), [arXiv:1512.02472 [hep-ph]].
 - [11] D. Barducci, G. Blanger, C. Hugonie and A. Pukhov, JHEP **1601**, 050 (2016), [arXiv:1510.00246 [hep-ph]].

- [12] U. Ellwanger and C. Hugonie, *JHEP* **1408**, 046 (2014), [arXiv:1405.6647 [hep-ph]].
- [13] U. Ellwanger and A. M. Teixeira, *JHEP* **1410**, 113 (2014), [arXiv:1406.7221 [hep-ph]].
- [14] J. Cao, C. Han, L. Wu, P. Wu and J. M. Yang, *JHEP* **1405**, 056 (2014), [arXiv:1311.0678 [hep-ph]].
- [15] J. Cao, K. i. Hikasa, W. Wang, J. M. Yang, *Phys. Lett. B* **703**, 292 (2011), [arXiv:1104.1754 [hep-ph]].
- [16] S. Kraml, A. R. Raklev and M. J. White, *Phys. Lett. B* **672**, 361 (2009), [arXiv:0811.0011 [hep-ph]].
- [17] F. Ferrer, L. M. Krauss and S. Profumo, *Phys. Rev. D* **74**, 115007 (2006), [hep-ph/0609257].
- [18] V. Barger, P. Langacker and G. Shaughnessy, *Phys. Lett. B* **644**, 361 (2007), [hep-ph/0609068].
- [19] J. F. Gunion, D. Hooper and B. McElrath, *Phys. Rev. D* **73**, 015011 (2006), [hep-ph/0509024].
- [20] R. Barbieri, L. J. Hall, A. Y. Papaioannou, D. Pappadopulo and V. S. Rychkov, *JHEP* **03**, 005 (2008), [arXiv:0712.2903 [hep-ph]].
- [21] S. Zheng, *Eur. Phys. J. C* **75**, no. 5, 195 (2015), [arXiv:1405.6907 [hep-ph]].
- [22] D. J. Miller, R. Nevzorov and P. M. Zerwas, *Nucl. Phys. B* **681**, 3 (2004). [hep-ph/0304049].
- [23] K. S. Jeong, Y. Shoji and M. Yamaguchi, *JHEP* **1204**, 022 (2012), arXiv:1112.1014 [hep-ph].
- [24] K. J. Bae, K. Choi, E. J. Chun, S. H. Im, C. B. Park and C. S. Shin, *JHEP* **1211**, 118 (2012). [arXiv:1208.2555 [hep-ph]].
- [25] U. Ellwanger and C. Hugonie, *Comput. Phys. Commun.* **175**, 290 (2006), [hep-ph/0508022].
- [26] G. Belanger, F. Boudjema, A. Pukhov and A. Semenov, *Comput. Phys. Commun.* **192**, 322 (2015), arXiv:1407.6129 [hep-ph].
- [27] D. S. Akerib *et al.* [LUX Collaboration], *Phys. Rev. Lett.* **118**, no. 2, 021303 (2017), [arXiv:1608.07648 [astro-ph.CO]].
- [28] D. S. Akerib *et al.* [LUX Collaboration], *Phys. Rev. Lett.* **116**, no. 16, 161302 (2016), [arXiv:1602.03489 [hep-ex]].
- [29] E. Aprile *et al.* [XENON Collaboration], *Phys. Rev. Lett.* **119**, no. 18, 181301 (2017), [arXiv:1705.06655 [astro-ph.CO]].
- [30] P. Cushman *et al.*, [arXiv:1310.8327 [hep-ex]].
- [31] D. S. Akerib *et al.* [LZ Collaboration], [arXiv:1509.02910 [physics.ins-det]].
- [32] S. Schael *et al.* [ALEPH and DELPHI and L3 and OPAL and SLD Collaborations and LEP Electroweak Working Group and SLD Electroweak Group and SLD Heavy Flavour Group], *Phys. Rept.* **427**, 257 (2006), [hep-ex/0509008].
- [33] G. Aad *et al.* [ATLAS and CMS Collaborations], *JHEP* **1608**, 045 (2016). [arXiv:1606.02266 [hep-ex]].
- [34] J. Cao, Y. He, L. Shang, W. Su and Y. Zhang, *JHEP* **1608**, 037 (2016), [arXiv:1606.04416 [hep-ph]].
- [35] V. Khachatryan *et al.* [CMS Collaboration], [arXiv:1701.01954 [hep-ex]].
- [36] P. A. R. Ade *et al.* [Planck Collaboration], *Astron. Astrophys.* **594**, A13 (2016), [arXiv:1502.01589 [astro-ph.CO]].
- [37] D. Das and U. Ellwanger, *JHEP* **1009**, 085 (2010), [arXiv:1007.1151 [hep-ph]].
- [38] G. Belanger, F. Boudjema, C. Hugonie, A. Pukhov and A. Semenov, *JCAP* **0509**, 001 (2005), [hep-ph/0505142].
- [39] A. Falkowski, F. Riva and A. Urbano, *JHEP* **1311**, 111 (2013), [arXiv:1303.1812 [hep-ph]].